Spatial Dynamics of Flood Hazard and Vulnerability: A Geostatistical and Google Earth Engine Approach in Eastern Kasur, Pakistan

Hira Shahbaz, Shahid Karim, Huda Arif
Department of Geography, Government College University Lahore, Lahore, Pakistan
*Correspondence: shahidkarim@gcu.edu.pk, hira72370@gmail.com

Citation | Shahbaz. H, Karim. S, Arif. H, "Spatial Dynamics of Flood Hazard and Vulnerability: A Geostatistical and Google Earth Engine Approach in Eastern Kasur, Pakistan", IJIST, Vol. 8 Issue. 1 pp 382-405, February 2026
Received | January 06, 2026 **Revised |** February 07, 2026 **Accepted |** February 09, 2026 **Published |** February 13, 2026.

Floods are among the most recurrent and destructive natural hazards, particularly in monsoon-dominated regions. This study presents a geospatial and geostatistical assessment of flood hazard, vulnerability, and resilience in eastern Kasur District, Pakistan, along the Sutlej River. A total of 150 households were surveyed using stratified random sampling, and results were integrated with Sentinel-1 and Sentinel-2 satellite imagery processed in Google Earth Engine (GEE). Spatial techniques, including Inverse Distance Weighted (IDW) interpolation, Anselin Local Morans I, Spatial Autocorrelation (Morans I) and linear regression, were applied. Results indicate that 17 km² of land was inundated, with agriculture accounting for 87.18% of the affected area, followed by built-up land (4.45%). Significant spatial clustering was observed for key vulnerability indicators, including household damage (Moran's I = 0.29, $p < 0.001$) and agricultural land erosion (Moran's I = 0.354, $p < 0.000001$). Economic losses reached PKR 250,000–400,000 per household, with income reductions up to 75%, while post-flood inflation exceeded 50% in hotspot areas. Regression analysis showed moderate spatial dependence ($R^2 = 0.1362$ and 0.1235), indicating both spatial and local drivers of vulnerability. Hotspot analysis identified Sahgerah, Wallay Wala, Ullanke & Jumeke, Maste Ki, Chanda Singh Wala, and Nagar Amanpura as high-risk clusters exhibiting multi-dimensional vulnerability. The Random Forest classifier demonstrated strong performance, achieving an overall accuracy of 86% and a Kappa coefficient of 0.82. The study demonstrates that integrating geostatistics with cloud-based remote sensing enables precise identification of flood vulnerability hotspots and supports targeted, data-driven flood risk management strategies.

Keywords: Flood Hazard, Eastern Kasur, GEE, Sentinel, Spatial Clustering, Vulnerability, Resilience

Introduction:

Climate change has increasingly intensified the frequency and magnitude of hydro-meteorological disasters, especially floods [1][2][3][4]. Floods are one of the most catastrophic natural disasters, occurring when water from a river or stream overflows and spreads over the flood plain, becoming a hazard to society [5][6][7]. The impacts of floods are increasing globally, not only due to climate change and global warming but also to rapid urbanization and the expansion of human settlements into floodplain areas, which significantly increase exposure and vulnerability to flood hazards [8][9]. Recent research highlights that flood risk is no longer viewed as a purely hydrological phenomenon but as a multi-dimensional process shaped by the interaction of hazard, exposure, and socio-economic vulnerability [10]. Contemporary studies emphasize that climate change, rapid urbanization, and land-use transformations are intensifying both the spatial extent and socio-economic impacts of floods, particularly in developing regions [9] [10]. Between 1998 and 2015, floods affected approximately 2.3 billion people worldwide, with Asia experiencing nearly 95% of these impacts. Riverine flooding currently affects about 21 million people annually, and due to climate change and rapid socio-economic development, this number is projected to rise to nearly 54 million by 2030 [11][12][13][14]. The 2020 flood in France resulted in the collapse of hundreds of bridges, roads, and residential buildings, while the recent flood in the US affected about 75,000 people, forcing them to leave their homes [15]. Developing countries such as Pakistan have historically experienced recurrent flooding from the Indus River and its tributaries. Major flood events recorded in 1955, 1973, 1976, 1988, 1992, and 1996 illustrate the destructive nature of these floods and their significant impacts on lives, infrastructure, and socio-economic systems [16][17][18][19][20]. The impacts of floods are magnified by limited adaptive capacity, weak governance, and resource constraints. Punjab province, traversed by five major rivers and characterized by extensive agricultural landscapes and dense population, is highly vulnerable to recurrent flooding, which significantly affects livelihoods, infrastructure, and regional socio-economic stability [21][22][23]. The most severe flood event in Pakistan's recent history occurred in 2010, affecting more than 20 million people and causing economic damages estimated at nearly 10 billion USD. This disaster highlighted the country's extreme vulnerability to large-scale hydrological hazards and the urgent need for improved disaster risk management and regional resilience [24][25][26]. The catastrophic floods of 2022 inundated nearly one-third of Pakistan after unprecedented monsoon rainfall broke a 30-year record, leading to 1,739 fatalities, affecting about 33 million people, and causing economic losses of nearly 30 billion USD in agriculture, fisheries, housing, transport, and food systems [27][28]. Among these areas, the Sutlej River floodplain in eastern Kasur District is recognized as one of the most flood-prone regions, historically experiencing recurrent and severe flooding due to its low-lying geomorphology, river dynamics, and transboundary hydrological influences [29][30]. The Sutlej River has historically experienced multiple severe flood events, with major occurrences recorded in 1995, 2010, 2019, 2023, and most recently in 2025. These events have repeatedly caused extensive damage to human settlements, infrastructure, and agricultural lands, highlighting the vulnerability of the region to hydrological hazards [29][31]. Most rural households in this district depend heavily on agriculture and livestock for livelihood, which amplifies the economic vulnerability of these communities.

Following a flood, the rapid and accurate assessment of crop damage is essential for government authorities and insurance providers to ensure timely relief and compensation. Such assessments also play a key role in guiding post-disaster recovery, improving flood management strategies, and mitigating future losses [32][33]. Traditional methods for flood damage assessment primarily depended on manual, on-the-ground surveys. Although widely used, these approaches are often slow, resource-intensive, subject to human error, and impractical for assessing large, remote, or heavily inundated areas, limiting their effectiveness

in timely disaster response [34][35][36]. Remote sensing provides a powerful tool for multi-resolution flood-inundation mapping and detailed flood risk assessment, supporting timely disaster preparedness, mitigation, and post-event relief efforts. Advanced methodologies now combine GIS, machine learning, deep learning, and fog computing-based real-time monitoring to enable accurate hazard mapping, rapid flood detection, and early warning systems across diverse geographic regions [37][38][14][39]. In comparison with traditional ground-based approaches, space-based sensors offer near-real-time and high-resolution monitoring of flood extent and dynamics. These technologies enable timely hazard assessment, support rapid disaster response, and enhance overall flood risk management strategies [40][41][42]. Monitoring and assessing the effects of floods across multiple river basins increasingly relies on optical satellite imagery, radar data, and derived flood products. Such Earth Observation-based approaches provide high-resolution, near-real-time insights into flood extent, dynamics, and impacts, supporting accurate mapping, forecasting, and improved risk management strategies at both regional and global levels [43][44][45]. Over the past decade, two dominant methodological approaches have emerged in flood risk assessment: remote sensing-based hazard mapping and socio-economic vulnerability analysis. Remote sensing techniques, particularly those utilising multi-sensor datasets such as Sentinel-1 Synthetic Aperture Radar (SAR) and Sentinel-2 optical imagery, enable high-resolution and near-real-time flood monitoring, even under cloud-covered conditions, thereby improving the accuracy of inundation mapping and disaster response. Recent advancements further integrate machine learning and hydrodynamic modeling with remote sensing to enhance predictive flood susceptibility and risk estimation [46][47]. However, despite their technical strengths, these approaches often focus primarily on physical flood extent and fail to adequately capture localized socio-economic dynamics, including livelihood disruption, adaptive capacity, and institutional response mechanisms. Several studies highlight the crucial role of Synthetic Aperture Radar (SAR) data in flood monitoring, owing to its ability to penetrate clouds and rainfall, providing accurate and near-real-time assessment of flood extent during and after events. SAR-based analyses are highly effective for distinguishing inundated areas from land, enabling rapid flood damage assessment, support for evacuation planning, and post-disaster recovery and reconstruction mapping [48][49][50]. In contrast, socio-economic approaches provide critical insights into community-level vulnerability by incorporating indicators such as income loss, access to services, and resilience capacity. Studies have demonstrated that socio-economic vulnerability significantly influences the severity and recovery trajectory of flood impacts, particularly in densely populated and resource-constrained regions [51]. While these approaches offer valuable depth, they are often limited by data subjectivity, lack of spatial continuity, and challenges in scaling to regional or national levels. Consequently, recent literature strongly advocates for integrated frameworks that combine geospatial technologies with socio-economic data to enable comprehensive flood risk assessment [52][53]. Despite these advancements, significant gaps remain in the integration and validation of such approaches. Many studies still treat hazard, vulnerability, and exposure as separate components, resulting in fragmented analyses that fail to capture the spatial interdependencies of flood risk. Recent research underscores the importance of spatial statistical techniques, such as Moran's I and cluster analysis, in identifying non-random patterns and localised hotspots of vulnerability, which are critical for targeted disaster risk reduction [54]. Furthermore, the emergence of cloud-based platforms such as Google Earth Engine (GEE) has revolutionised flood analysis by enabling large-scale data processing, multi-temporal analysis, and integration of machine learning models; however, their application in developing countries remains limited and often lacks integration with field-based socio-economic data [55].

In Pakistan, existing studies predominantly rely on either remote sensing-based flood mapping or conventional survey-based assessments, resulting in a lack of spatially explicit and

multi-dimensional frameworks. This limitation is particularly evident in flood-prone regions such as the Sutlej River floodplain in eastern Kasur, where recurring flood events demand more localized, data-driven, and integrated assessment approaches. Therefore, this study addresses these research gaps by developing a comprehensive geospatial and geostatistical framework that integrates multi-sensor remote sensing data processed in Google Earth Engine with household-level socio-economic information. By applying advanced spatial analytical techniques, including Inverse Distance Weighted (IDW) interpolation, Global and Local Moran's I, and regression analysis, the study moves beyond descriptive assessments to quantitatively evaluate spatial clustering and underlying drivers of vulnerability. This integrated approach enhances analytical depth, enabling the identification of statistically significant vulnerability hotspots and contributing to more effective, spatially targeted flood risk management strategies in high-risk rural environments. This provides a scalable, data-driven, and spatially explicit flood damage assessment framework for the Sutlej River corridor, overcoming the spatial, temporal, and logistical limitations of conventional methods. Hence, assessing resilience through geospatial and geostatistical approaches is vital for evidence- based flood risk management and the design of targeted adaptation strategies in high-risk rural regions like Eastern Kasur.

Despite significant advancements in flood risk assessment, several critical gaps remain in the existing literature. First, many studies rely predominantly on either remote sensing-based hazard mapping or socio-economic vulnerability assessments, with limited integration between cloud-based platforms such as Google Earth Engine (GEE) and household-level primary data. This lack of integration restricts the ability to capture both spatial flood dynamics and ground-level impacts within a unified analytical framework. Second, although geospatial techniques are widely applied, the use of robust spatial statistical validation methods—such as Global and Local Moran's I and hotspot analysis—remains limited, reducing the capacity to identify statistically significant clustering patterns and spatial dependencies in flood vulnerability. Third, existing research often focuses on regional or basin-scale assessments, with minimal attention to fine-scale, village-level vulnerability mapping, which is essential for targeted and localized disaster risk reduction. These limitations highlight the need for an integrated, spatially explicit, and statistically validated framework that combines multi-sensor remote sensing, geostatistical analysis, and socio-economic data. Therefore, this study addresses these gaps by developing a village-scale flood vulnerability assessment approach that integrates GEE-based flood mapping with household survey data and advanced spatial statistical techniques to identify and validate vulnerability hotspots in eastern Kasur.

Research Objectives:

To quantify flood extent and land-cover impact using Sentinel-based imagery in GEE.

To evaluate the spatial clustering of flood vulnerability indicators using Moran's I and hotspot analysis.

To model relationships between spatial clustering and vulnerability using regression analysis.

To delineate flood vulnerability hotspots for targeted risk reduction.

Novelty statement:

This study advances existing flood vulnerability research by integrating household-level socio-economic data with cloud-based multi-sensor remote sensing (SAR + optical) and validated geostatistical techniques. Unlike previous studies, which focus on either hazard mapping or socio-economic assessment, this research provides a multi-dimensional, spatially validated, and village-scale framework. The inclusion of Moran's I-based clustering and regression validation further strengthens its novelty by quantifying spatial dependence in vulnerability patterns.

Material and Methods:

Study Area:

The study area Figure 1 is located in eastern Kasur District, Punjab, Pakistan, along the Sutlej River floodplain near the Pakistan–India border, approximately 55 km south of Lahore (31.12° N, 74.44° E), with elevations ranging from 150 to 200 m above sea level. Covering about 3,995 km², the district is bounded by Lahore to the north, Okara to the south, India to the east, and Nankana Sahib to the northwest [56]. Administratively, Kasur comprises four tehsils—Kasur, Chunian, Kot Radha Kishan, and Pattoki—with 125 union councils and 10 towns, and the study focused on flood-prone villages in Chunian and Kasur tehsils, including Fatuhi Wala, Ganda Singh, Jumay Kay, Ullanke, Chanda Singh Wala, Sahgerah, and Huseen Khane. Topographically, the region lies within the lower Sutlej sub-basin, characterised by flat terrain, low relief, and concentrated runoff, directing floodwaters toward the riverine plains and aggravating waterlogging during monsoon rainfall or upstream releases. Kasur experiences a semi-arid climate with hot summers (up to 40°C), mild winters (6–20°C), and an average annual rainfall of 500 mm [57]. With a population of over 4 million, predominantly rural and agrarian, settlements along the floodplain are highly vulnerable to socioeconomic losses during floods. In 2025, water levels at the Ganda Singh Wala gauging station reached a 35-year high on August 19, highlighting the region's acute flood risk (National Disaster Management Authority, 2025). The country's chief meteorologist for flood monitoring noted that the river had reached its highest level in the past 35 years, highlighting the severity of flooding in this region and underscoring the need for a detailed flood damage assessment.

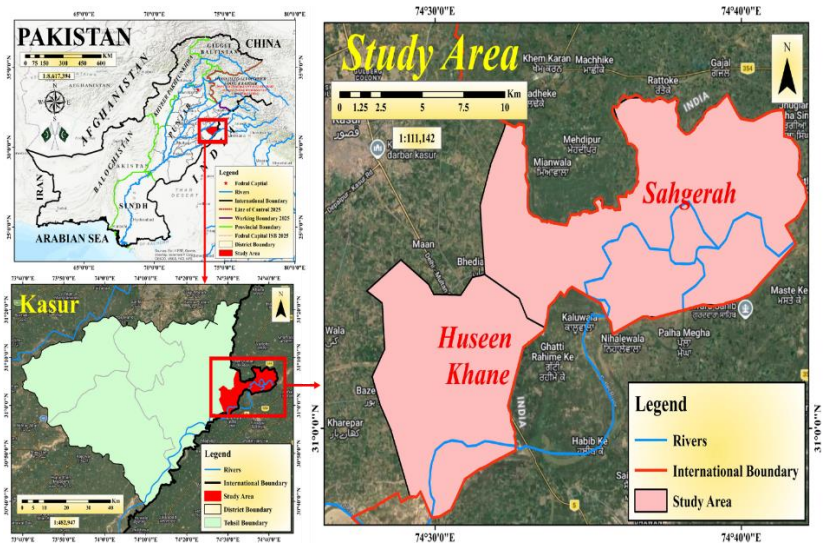

Figure 1. Study Area Map

Figure 2 illustrates the integrated methodological framework adopted in this study, which combines remote sensing, geospatial analysis, and field-based socio-economic data to assess flood hazard and vulnerability in eastern Kasur. The framework is structured into four main phases: data acquisition, preprocessing, spatial analysis, and integration with validation.

In the first phase, both primary and secondary datasets were collected. Primary data were obtained through household surveys using a stratified random sampling approach, capturing information on physical damage, socio-economic conditions, and adaptive capacity. Secondary data included multi-sensor satellite imagery, specifically Sentinel-1 SAR for flood inundation mapping and Sentinel-2 optical data for post-flood land cover analysis, processed within the Google Earth Engine (GEE) environment [58][59]

The second phase involved data preprocessing, where satellite imagery was filtered, corrected, and classified, while survey data were coded and georeferenced using GPS

coordinates. This ensured spatial compatibility between field-based and remotely sensed datasets. In the third phase, spatial and geostatistical analyses were performed. Flood extent was delineated using SAR-based thresholding techniques in GEE, while land cover classification was conducted using a Random Forest algorithm. To assess spatial patterns of vulnerability, Inverse Distance Weighted (IDW) interpolation was applied to generate continuous surfaces of key indicators. Spatial autocorrelation was evaluated using Global Moran's I to identify overall clustering patterns, and Anselin Local Moran's I was used to detect hotspots and cold spots of vulnerability. Additionally, regression analysis was conducted to examine the relationship between spatial clustering and vulnerability indicators. In the final phase, results from remote sensing and survey-based analyses were integrated within a GIS environment (ArcGIS Pro 3.2) to produce spatially explicit flood vulnerability maps. Validation was carried out using a confusion matrix approach to assess classification accuracy, including overall accuracy and the Kappa coefficient. This integrated framework enables a comprehensive, multi-dimensional assessment of flood hazard, exposure, and vulnerability, supporting data-driven and spatially targeted flood risk management.

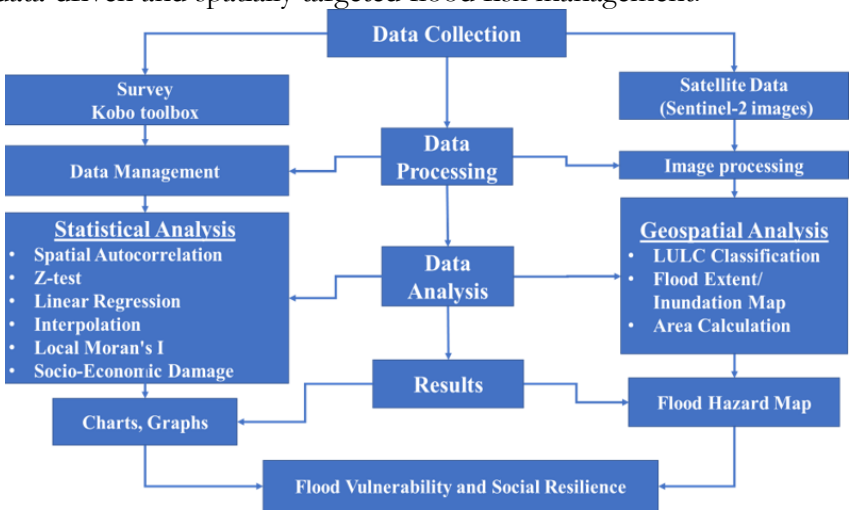

Figure 2. Methodological Framework

Survey-Based Data Collection:

This study used an integrated mixed-methods approach to evaluate flood inundation, flood-induced physical impacts, and post-flood land cover changes in the eastern Kasur villages along the Sutlej River in Punjab, Pakistan. Household surveys were used to gather primary data. To ensure sufficient representation across a range of geographic locations and socioeconomic circumstances, 150 representative households from rural and semi-urban settlements were chosen using a stratified random sampling technique. A sample size of 150 households was determined using standard sampling principles for spatial socio-economic studies, ensuring representation across villages and achieving a confidence level of approximately 95% with an acceptable margin of error for exploratory spatial analysis. In order to document both ground-level physical damage and its spatial manifestation, the methodological framework integrates field-based observations with quantitative analysis of satellite-based remote sensing and geospatial data. In order to guarantee analytical accuracy, a methodical survey implementation, preprocessing of remote sensing imagery, spatial modelling to define the extent of the flood and impacted areas, and geostatistical validation were carried out. The methodology supports evidence-based flood risk assessment and mitigation planning in highly flood-prone riverine environments by combining household-level survey data with GIS-based spatial analysis and Sentinel-2-derived post-flood land cover information to provide a spatially explicit and statistically robust assessment of flood-induced physical vulnerability.

Data Analysis:

To enable precise georeferencing, mobile applications (like Kobo Toolbox) were used to record the GPS coordinates of the households surveyed. To enable quantitative analysis, survey data were coded in Microsoft Excel using numerical codes for categorical variables (e.g., "Yes" = 1, "No" = 0; flood frequency: "Always" = 4 to "Never" = 1). For geospatial analysis, the dataset was loaded into ArcGIS Pro 3.2. The intensity and distribution of physical vulnerability were represented by continuous raster surfaces created using Inverse Distance Weighted (IDW) interpolation. IDW interpolation was performed using a power value of 2 and a variable search radius including 12 nearest neighbors, ensuring balanced spatial smoothing and minimizing interpolation bias. Anselin Local Moran's I was used to identify localized hotspots and cold spots, highlighting villages most at risk of flood damage, and Global Moran's I was used to assess spatial clustering to identify general spatial patterns. For regression analysis, the dependent variable represents the dependent variable represents the statistical significance of flood vulnerability indicators (Z-scores), while the independent variable represents spatial clustering intensity measured through Moran's I. This relationship was used to assess the extent to which spatial dependence explains variations in vulnerability patterns.

Post-Flood Land Cover Analysis:

Post-flood land cover impacts were evaluated using Sentinel-2 optical imagery processed via the Google Earth Engine (GEE) cloud platform in order to supplement field-based data [60][61]. The land cover dataset is based on Sentinel-2 imagery (10 m resolution) and generated using a deep learning model developed by Impact Observatory and Esri. The dataset has undergone extensive global validation and demonstrates high classification accuracy. However, to ensure reliability at the local scale, an independent accuracy assessment was conducted using a confusion matrix. In order to assess the spatial extent of flood impacts, this made it possible to quantify the areas affected by flooding, identify residential areas, croplands, and vegetation damage, and integrate the results with the locations of villages.

Integration and Validation:

The mapping software ArcGIS Pro 3.2 was used to integrate survey-based physical vulnerability data and post-flood land cover maps derived from Sentinel-2. To verify patterns of physical damage and inundation, post-flood land cover was superimposed on IDW-generated raster surfaces and spatial clustering results. By tying together exposure at the household level, agricultural and structural damage, and flood impacts at the landscape level, this integrated approach offered a thorough evaluation of flood vulnerability.

Accuracy Assessment:

The accuracy of the classified satellite imagery was evaluated using a machine learning–based validation approach. A total of 723 reference polygons were generated, of which 80% (n = 602) were used for training, and 20% (n = 121) were reserved for testing and validation purposes. These samples were utilized to construct robust training and validation datasets within Google Earth Engine (GEE).

Classification accuracy was assessed using a confusion matrix, following standard practices in remote sensing [62]. The overall accuracy (OA) and Kappa coefficient (K) were computed to evaluate the performance of the Random Forest classifier. Overall accuracy represents the proportion of correctly classified pixels relative to the total number of pixels and is expressed as:

$$OA = (Pc / Pn) \times 100. \textbf{Eq. 1}$$

where Pc is the number of correctly classified pixels, and Pn is the total number of pixels.

The Kappa coefficient, which measures the agreement between classified and reference data while accounting for chance agreement, was calculated as:

$$K = [N \Sigma xii - \Sigma (xi+ \times x+i)] / [N^2 - \Sigma (xi+ \times x+i)]. \textbf{Eq.2}$$

where N is the total number of observations, xii represents correctly classified observations (diagonal elements), xi+ is the sum of row i, and x+i is the sum of column i in the error matrix.

In addition, class-specific accuracies were evaluated using Producer's Accuracy (PA) and User's Accuracy (UA). Producer's Accuracy indicates the probability of a reference pixel being correctly classified, while User's Accuracy reflects the reliability of the classified pixels for each class. These metrics also allow the assessment of omission and commission errors, thereby providing a comprehensive understanding of classification performance. The confusion matrix approach implemented in GEE ensures reliable validation of classification results, enabling the quantification of classification errors and the overall effectiveness of the Random Forest model.

Results and Discussion:

Flood Inundation:

Figure 3 shows that the total flood-inundated area in Eastern Kasur along the Sutlej River is 17 km², primarily affecting low-lying riverine zones. Agricultural land was the most impacted, covering 87.18% of the inundated area, causing significant crop damage and disruption to rural livelihoods. Built-up areas accounted for 4.45%, water bodies 3.01%, and barren land 1.73%. The use of Sentinel-1 and Sentinel-2 data on the Google Earth Engine allowed rapid and accurate mapping of flood extent, highlighting the need for targeted mitigation and community preparedness in vulnerable floodplain areas.

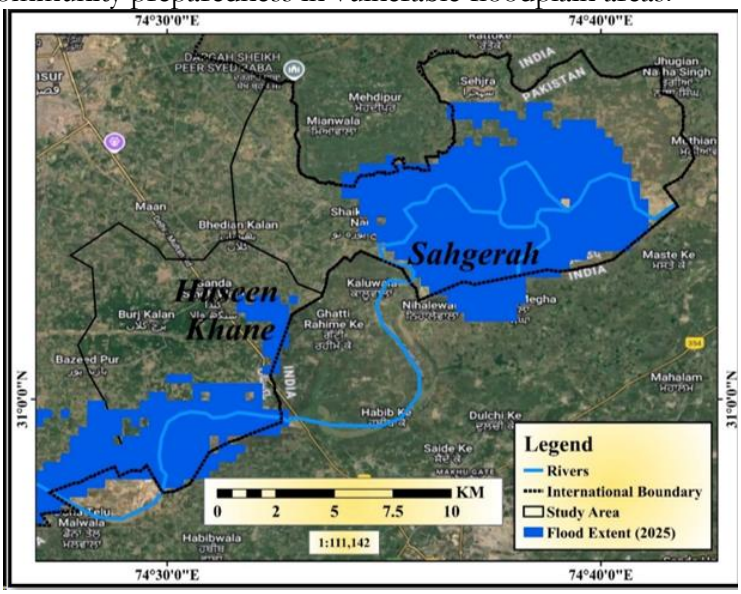

Figure 3. Flood Extent in Study Area (2025)

The first objective aimed to quantify flood extent and assess land-cover impacts using Sentinel-based imagery in Google Earth Engine (GEE). (Figure 4-5) highlights severe crop damage, livelihood disruption, and heightened food security risks in the region. Built-up areas (4.45%) experienced localized but significant damage to settlements and infrastructure, while water bodies (3.01%) and barren land (1.73%) were comparatively less affected. The identification of Sahgerah as the most critical high-risk hotspot underscores the need for prioritized intervention in this locality, including embankment strengthening, flood-resilient cropping systems, and community-based preparedness measures. This finding highlights the severe impact of flooding on agrarian livelihoods and regional food security. The dominance of agricultural loss reflects the vulnerability of low-lying floodplain areas, where subsistence farming is the primary source of income. The use of multi-sensor satellite data enabled accurate and rapid delineation of flood extent, supporting effective hazard assessment and response planning.

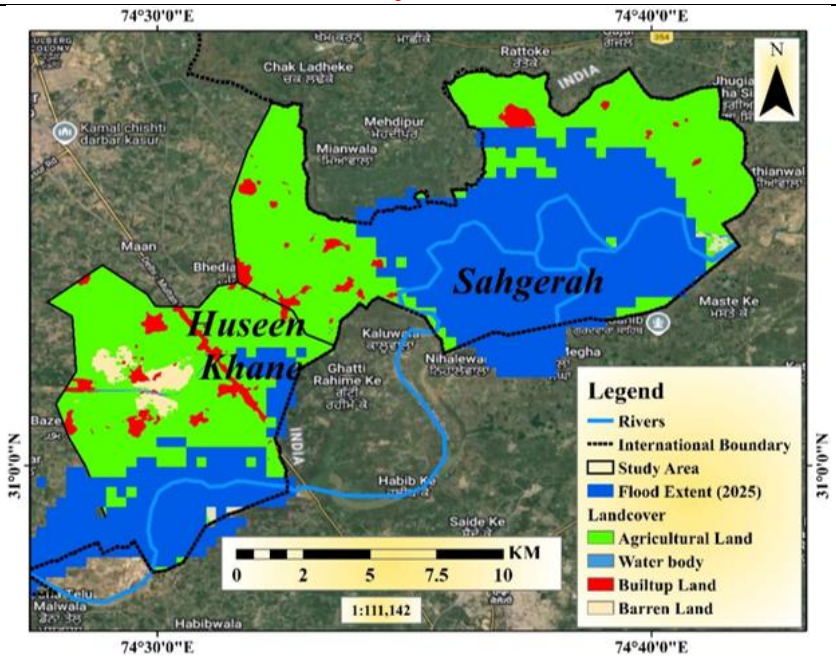

Figure 4. Affected Landcover

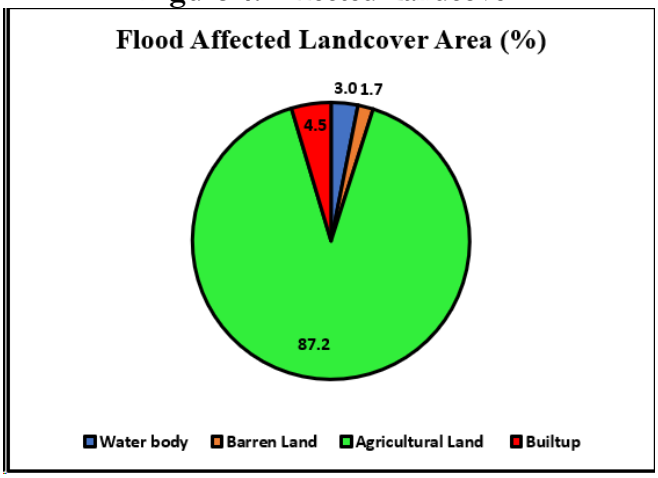

Figure 5. Graphical Representation of affected landcover area (%)

The accuracy assessment of the Random Forest classifier was performed using a confusion matrix derived from validation samples. The confusion matrix Table 1 shows that Built-up areas achieved a Producer's Accuracy of 92% and a user's Accuracy of 86%, indicating reliable classification with minor confusion with barren land. Water bodies exhibited the highest classification reliability (UA = 100%, PA = 95%), while Barren land also showed high accuracy (UA = 90%, PA = 90%). The results Table 2 indicate an overall accuracy of 0.86 and a Kappa coefficient of 0.82, demonstrating strong agreement between classified and reference data. These results confirm that the Random Forest classifier performs effectively for land cover classification in the study area.

Table 1. Confusion matrix for accuracy assessment of random forest classification

Reference \ Classified	Built-up	Water	Barren Land	Row Total	Producer's Accuracy (%)
Built-up	12	0	1	13	92
Water	1	18	0	19	95
Barren Land	1	0	9	10	90
Column Total	14	18	10	42	

User's Accuracy (%)	86	100	90		

Table 2. Accuracy assessment for Random Forest classification

Classifier	Data Source	Overall Accuracy (OA)	Kappa Coefficient (κ)
RF	Sentinel-2 (2025)	0.86	0.82

Physical–Environmental Vulnerability:

Damage Assessment:

The second objective focused on assessing the spatial clustering of flood vulnerability indicators using geostatistical techniques. The results demonstrate statistically significant spatial autocorrelation across multiple indicators. Household damage exhibited a Moran's I value of 0.29 ($p < 0.001$), while agricultural land erosion showed even stronger clustering (Moran's I = 0.354, $p < 0.000001$), confirming that flood impacts are spatially non-random. Hotspot analysis identified Sahgerah, Wallay Wala, Ullanke & Jumeke, Maste Ki, Chanda Singh Wala, and Nagar Amanpura as major high-risk clusters. These areas consistently exhibited high values across physical, structural, and socio-economic vulnerability indicators.

Figure 8 illustrating clustering of floodwater entry frequency (Moran's I = 0.318) and lack of structural adaptation (Moran's I = 0.277) further indicates repeated exposure and inadequate preparedness Household damage shows strong positive spatial autocorrelation (Moran's I = 0.290, Z = 4.38, p = 0.000012), with IDW interpolation indicating severe destruction in low-lying areas where flood depths exceeded 2 meters and reconstruction costs ranged from PKR 80,000 to 200,000 per dwelling. Agricultural land erosion displays even stronger clustering (Moran's I = 0.354, Z = 5.90, $p < 0.000001$), forming linear corridors along the river and causing 30–50% loss of cultivable land. The presence of High-High clusters, along with High-Low and Low-High outliers, confirms that damage is concentrated in specific locations, emphasizing the need for prioritized intervention, emergency response, and targeted flood risk reduction measures in these critical hotspots. These findings confirm that flood vulnerability is geographically concentrated, emphasizing the importance of spatial analysis in identifying priority intervention zones.

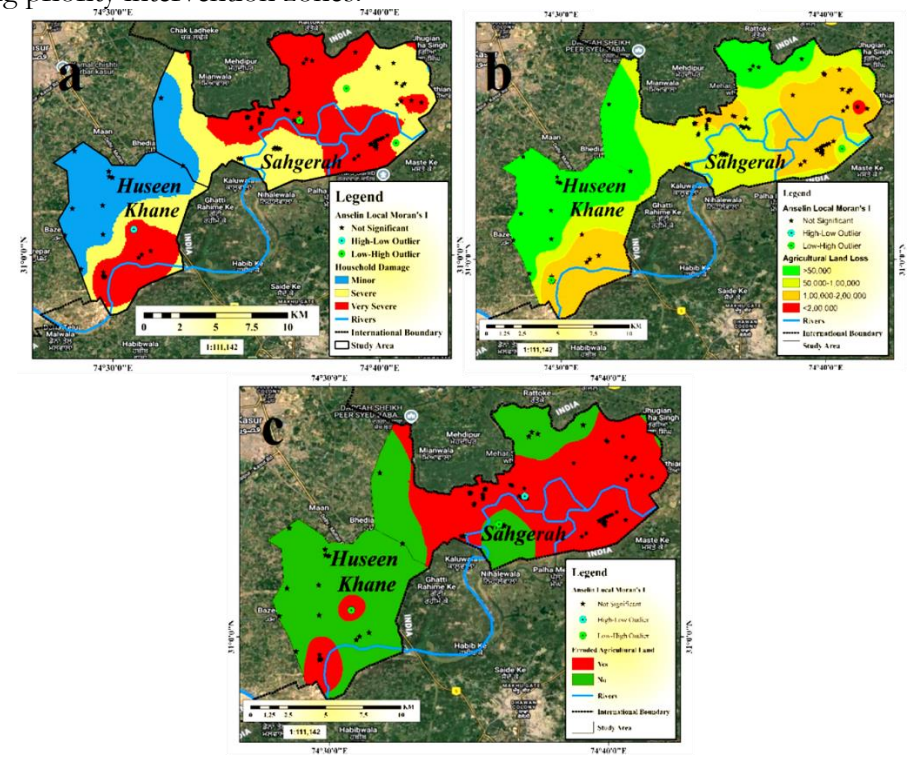

Figure 6. Damage indicators representing the actual impact of floods, categorized as (a) Household Damage, (b) Agricultural Land Loss, and (c) Agricultural Land Erosion.

Structural Vulnerability and Flood Exposure:

The spatial analysis of settlements along the Sutlej River floodplain in eastern Kasur reveals distinct patterns of structural vulnerability and flood exposure Figure 7. Housing conditions are predominantly Katcha (mud) and Semi-Pucca, yet the spatial distribution of structural fragility is statistically random (Moran's I = 0.029, Z = 0.61, p = 0.5379), indicating that structural weakness is uniformly distributed across the surveyed villages. In contrast, floodwater entry frequency exhibits strong spatial clustering (Moran's I = 0.318, Z = 4.80, p = 0.000001), with recurring intrusion hotspots concentrated in southern Sahgerah and Huseen Khane due to low-lying topography and inadequate drainage infrastructure. Significant clustering of households lacking structural modifications—such as raised plinths or reinforced walls—is observed in Sahgerah, Wallay Wala, Ullanke & Jumeke, Maste Ki, Chanda Singh Wala, and Nagar Amanpura, aligning closely with areas experiencing repeated floodwater entry (Moran's I = 0.277, Z = 4.17, p = 0.000029). IDW surfaces further confirm that proactive flood-proofing measures are largely absent in these high-exposure zones, reflecting economic constraints and limited technical knowledge among residents. Collectively, these findings identify critical structural vulnerability hotspots across eastern Kasur, which should be prioritized for targeted retrofitting, community-based flood resilience, and adaptive intervention strategies.

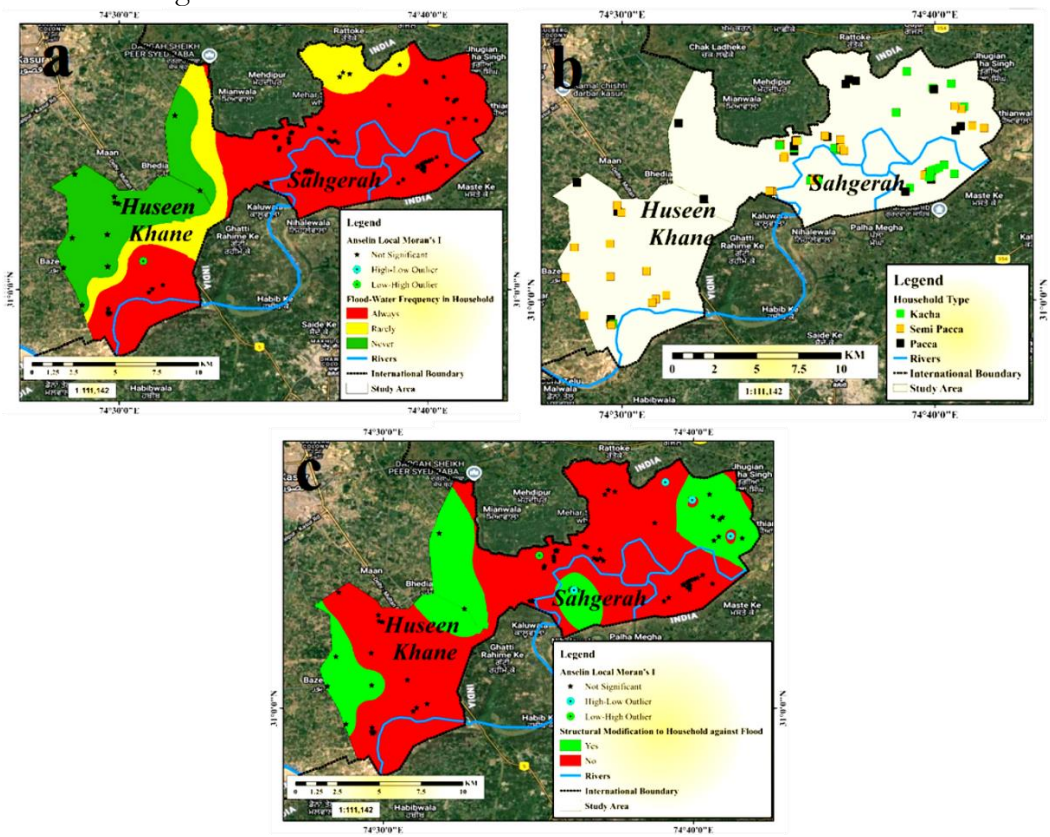

Figure7. Exposure indicators representing the likelihood of being affected by floods, categorized as (a) Flood Inundation Frequency, (b) Housing Structure, and (c) Structural Adaptation Measures

Socio-Economic Vulnerability:

Geospatial analysis of the 2025 flood in eastern Kasur reveals clustered social vulnerability (Figure 8). Households lacking potable water were concentrated in southern and eastern Sahgerah, Wallay Wala, Ullanke & Jumeke, Maste Ki, Chanda Singh Wala, and Nagar Amanpura (Moran's I = 0.291, Z = 4.39, p = 0.000011), with floodwater contaminating wells and hand pumps, increasing risk of waterborne diseases. Rescue service inaccessibility also

clustered in central and eastern Sahgerah (Moran's I = 0.173, Z = 2.71, p = 0.007225), highlighting institutional response gaps. The overlap of water scarcity and limited emergency support underscores acute multi-dimensional vulnerability, stressing the need for targeted rescue infrastructure and improved access to basic services.

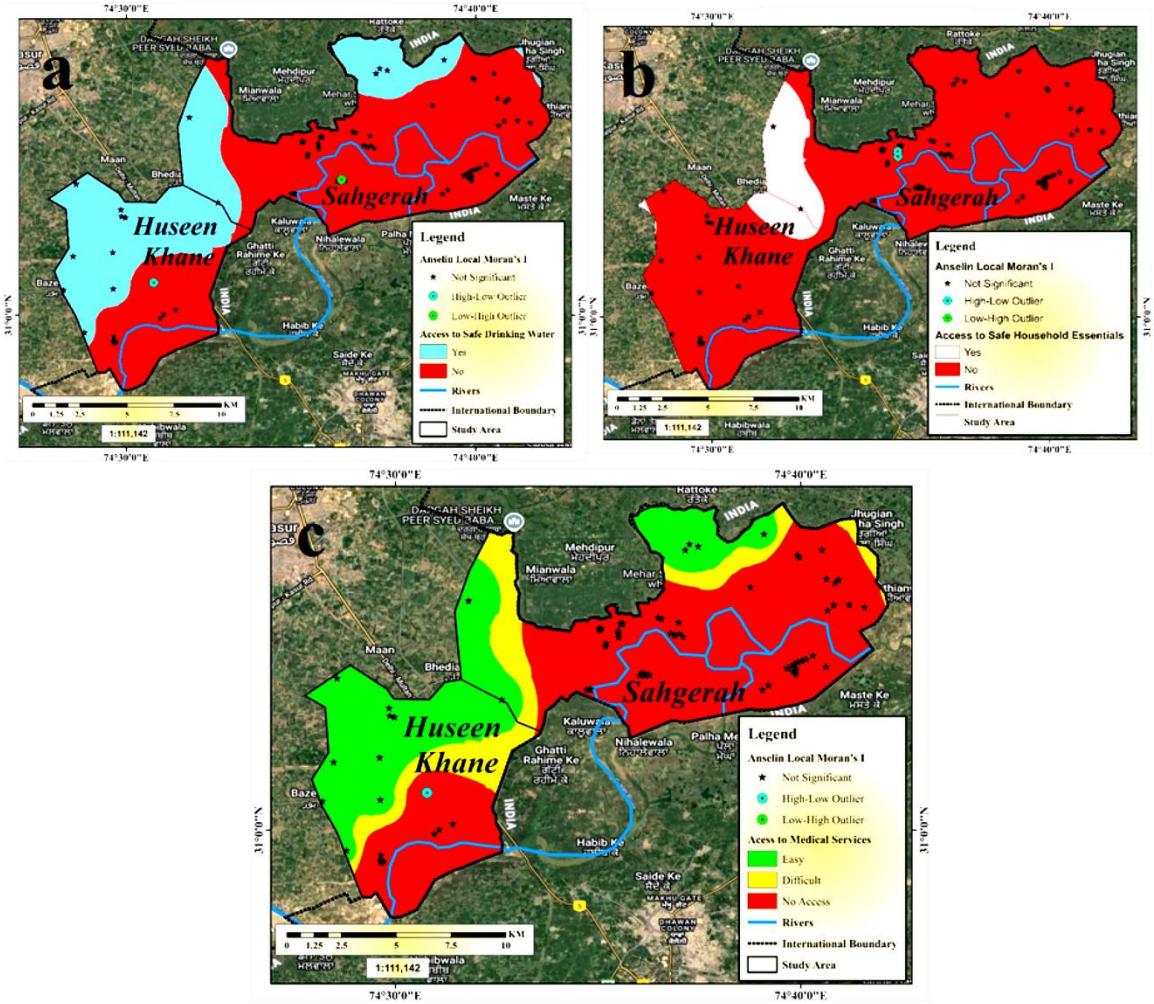

Figure 8. Access to Basic Services indicators as (a) Access to Safe Water, (b) Access to Health Services, and (c) Price Inflation during Flood.

Economic Vulnerability:

The geospatial analysis Figure 9 of the 2025 flood in eastern Kasur shows strong spatial clustering of income loss (Moran's I = 0.284, Z = 4.27, p = 0.000019), with households in western Huseen Khane, Sahgerah, Wallay Wala, Ullanke & Jumeke, Maste Ki, Chanda Singh Wala, and Nagar Amanpura losing up to 75% of their income (PKR 250,000–400,000). Flood exposure aligns with high-intensity loss zones, while livestock losses were randomly distributed (Moran's I = −0.021, Z = −0.12, p = 0.90064) due to preemptive coping. Post-flood inflation clustered in northeastern Sahgerah (Moran's I = 0.494, Z = 8.15, p < 0.000001), with essential goods prices rising over 50%. These settlements are key economic vulnerability hotspots, emphasizing the need for targeted livelihood support, financial recovery, and market stabilization.

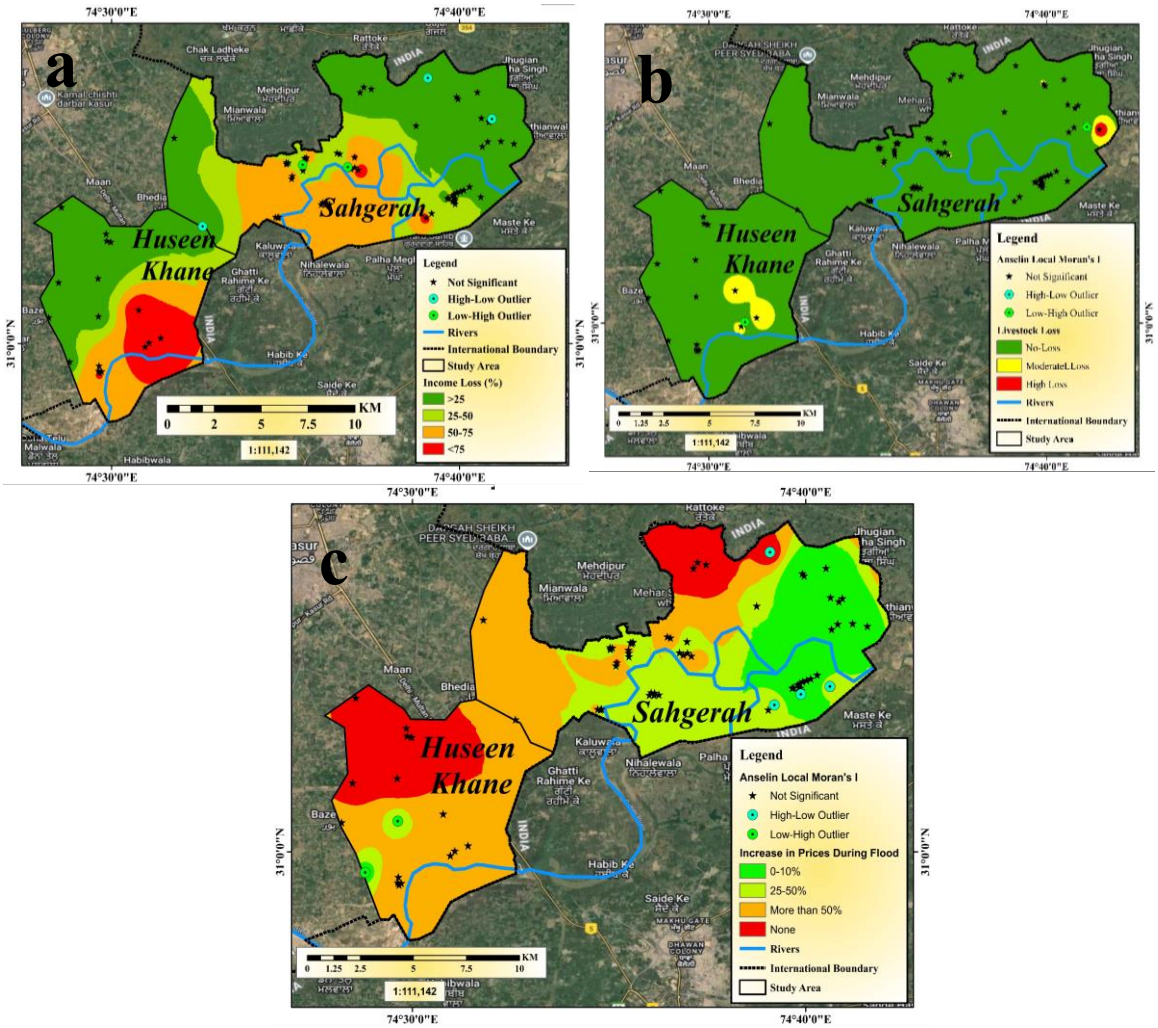

Figure 9. Economic Vulnerability indicators categorized as (a) Income Loss, (b) Livestock Loss, and (c) Price Inflation during Flood.

Social Resilience & Adaptive Capacity:

The geospatial analysis Figure 10 shows significant clustering of households lacking early flood warnings (Moran's I = 0.305, Z = 4.63, p = 0.000006) in southern Sahgerah, Wallay Wala, Ullanke & Jumeke, Maste Ki, Chanda Singh Wala, and Nagar Amanpura, highlighting communication gaps and delayed evacuation. Temporary relocation facilities clustered in the western highlands (Moran's I = 0.285, Z = 4.29, p = 0.000018), revealing geographic inequalities in emergency shelter access. Community preference for long-term structural adaptation strongly clustered (Moran's I = 0.670, Z = 11.08, p = 0.000000) in the same floodplain settlements, favoring dams and embankments over non-structural approaches. These patterns indicate multi-dimensional resilience deficits, emphasizing the need for improved early warning, accessible evacuation, and integrated adaptation strategies.

Flood Vulnerability Hotspots:

The final objective focused on identifying flood vulnerability hotspots for targeted risk reduction. The integrated geospatial analysis (Figure 11) revealed significant High–High clusters, indicating areas with consistently high vulnerability across multiple indicators. The results identify Sahgerah, Wallay Wala, Ullanke & Jumeke, Maste Ki, Chanda Singh Wala, and Nagar Amanpura as the major vulnerability hotspots, falling under zones of severe flood damage and exhibiting consistently high risk across all assessed indicators, including physical exposure, economic loss, and social vulnerability. The presence of pronounced High-High

clusters confirms concentrated pockets of extreme vulnerability, while High-Low and Low-High outliers highlight areas with atypical risk patterns relative to their surroundings. The identification of these hotspots demonstrates that flood impacts are multi-dimensional and spatially concentrated. These findings provide a strong basis for targeted interventions, including infrastructure development, community-based disaster risk management, and policy prioritization. This spatial configuration demonstrates that flood impacts are not randomly distributed but are intensely localized within specific settlements, reinforcing the cumulative effect of repeated flood exposure, weak infrastructure, and limited adaptive capacity. Collectively, these findings delineate critical priority zones for targeted flood risk management, enhanced emergency preparedness, and the implementation of long-term, integrated adaptation strategies.

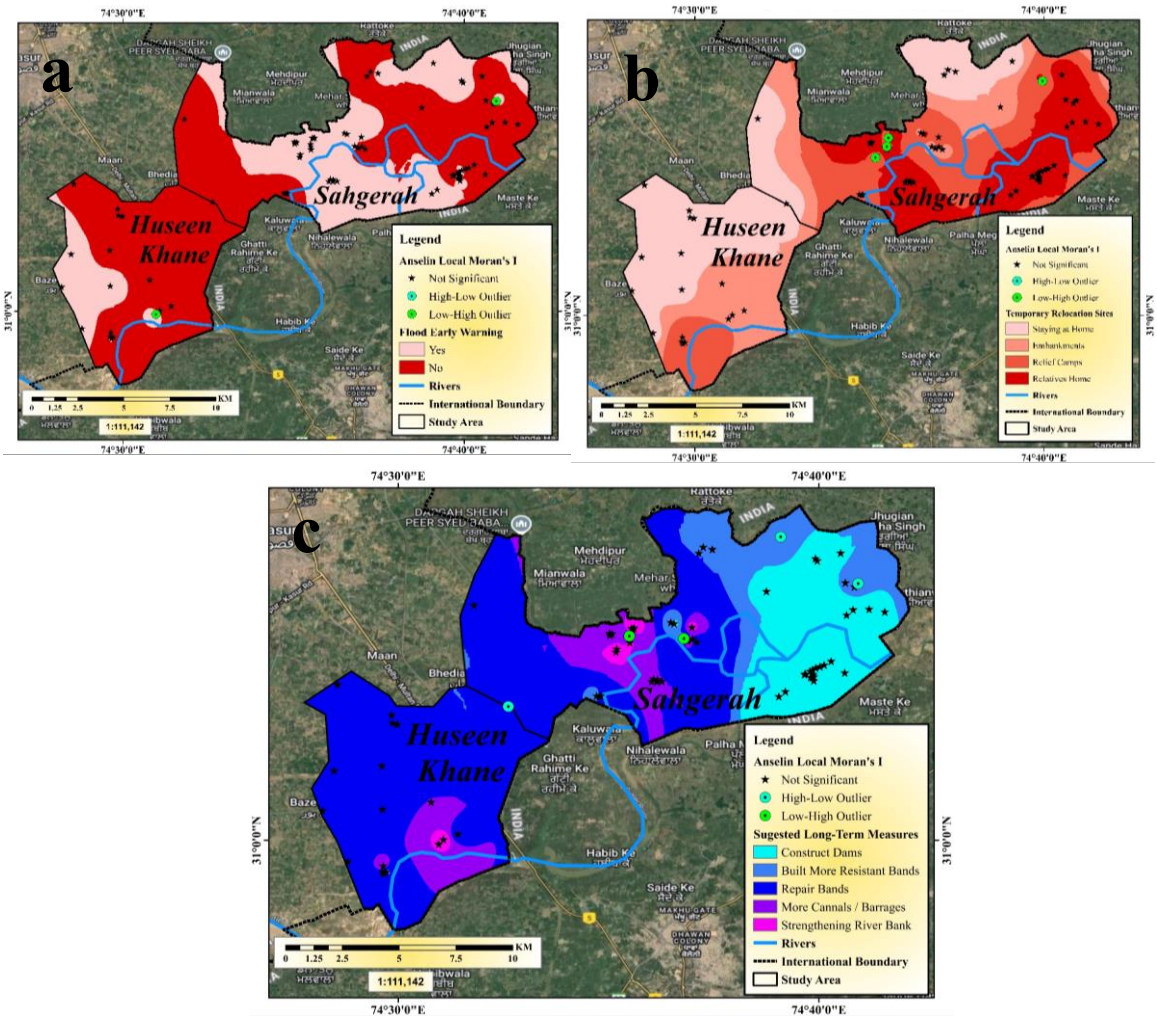

Figure 10. (a) Preparedness: Flood Early Warning, (b) Response: Temporary Relocation Facilities, and (c) Recovery: Long-term Adaptation Measures

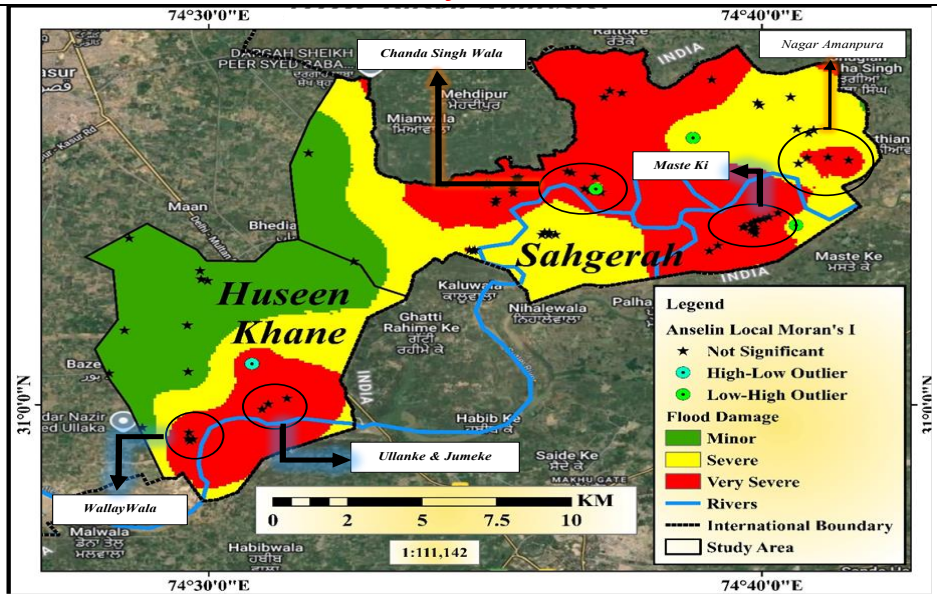

Figure 11. Flood Vulnerability and Hotspots Identification

The third objective aimed to examine the relationship between spatial clustering and vulnerability indicators using regression analysis. Table 3 shows a positive relationship between Moran's I values and statistical significance (Z-scores), indicating that areas with stronger spatial clustering tend to exhibit higher vulnerability levels. The Linear regression analysis demonstrates a positive relationship between spatial clustering and statistical significance across flood vulnerability indicators in the eastern floodplain of the Sutlej River (Figure 12). The regression model produced an R^2 value of 0.1362 (Z-test) and 0.1235 (Moran's I), suggesting that approximately 12–13% of the variation in vulnerability is explained by spatial clustering. Although the explanatory power is moderate, the positive slope confirms that spatial dependence contributes to the formation of vulnerability patterns. The regression analysis identified land use, population density, slope, proximity to rivers, and impervious surface area as key determinants of flood susceptibility. In contrast, slope was not statistically significant, suggesting that in this context, slope alone does not strongly influence flood occurrence. This result indicates that while spatial clustering plays an important role, flood vulnerability is also influenced by local socio-economic and environmental factors, highlighting the need for integrated analysis. This trend highlights that flood vulnerability in eastern Kasur is partially spatially dependent, while also influenced by local, non-spatial factors. Overall, the regression findings provide supporting evidence that spatial clustering contributes to the formation of vulnerability hotspots, reinforcing the need for geographically targeted flood risk management and planning strategies.

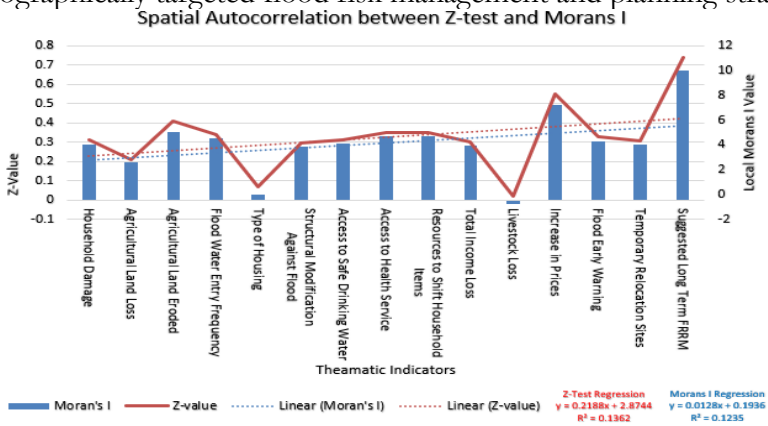

Figure 12. Graphical Representation of the Spatial Autocorrelation of Moran's I and the z-value of thematic variables

Table 3. Univariate for Key Flood Vulnerability and Impact Variables in the Study Area.

ID	Thematic Variable	Moran's I	Z-value	Significance of Clustering	Interpretation / Relationship
1	Household Damage	0.29	4.38	Significant Clustering	Direct impact: Severe housing damage concentrated in Sahgerah.
2	Agricultural Land Loss	0.194	2.84	Significant Clustering	Economic loss (PKR 100,000–200,000) is geographically concentrated.
3	Agricultural Land Eroded	0.354	5.9	Highly Significant Clustering	Localised erosion confirms concentrated fluvial hazard.
4	Flood Water Entry Frequency	0.318	4.8	Significant Clustering	Repeated water entry concentrated in hazard zones.
5	Type of Housing	0.029	0.61	Random Distribution	Widespread fragile structures; no single concentration.
6	Structural Modification Against Flood	0.277	4.17	Significant Clustering	Lack of modification clustered; low preparedness.
7	Access to Safe Drinking Water	0.291	4.39	Significant Clustering	Unsafe water access clustered; high health risk.
8	Access to Health Service	0.332	4.99	Significant Clustering	Clustered lack of health service availability.
9	Resources to Shift Household Items	0.332	4.99	Significant Clustering	Clustering of low preparedness to save assets.
10	Total Income Loss	0.284	4.27	Significant Clustering	Clustered income loss (>75%) confirms concentrated economic collapse.
11	Livestock Loss	-0.021	-0.12	Random Distribution	Individual asset loss; no clustered pattern.
12	Increase in Prices	0.494	8.15	Very Highly Significant Clustering	Localised inflation (>50%) in affected pockets.
13	Flood Early Warning	0.305	4.63	Significant Clustering	Lack of early warning is concentrated spatially.
14	Temporary Relocation Sites	0.285	4.29	Significant Clustering	Clustered use of camps and relatives' homes.
15	Suggested Long Term FRRM	0.67	11.08	Extremely High Clustering	Clustered belief in structural flood control (Dams/Barrages).

Discussion:

The present study provides a spatially explicit and integrated assessment of flood hazard and vulnerability in eastern Kasur, revealing strong clustering of flood impacts, extensive agricultural loss, and the emergence of multi-dimensional vulnerability hotspots. While many of these findings align with existing literature, a more critical comparison highlights both areas of agreement and important divergences. The dominance of agricultural land loss (87.18%) observed in this study is consistent with prior research in floodplain regions of Pakistan and South Asia, where agriculture is typically the most affected sector due to its location in low-lying and river-adjacent zones. Similar patterns have also been reported in studies highlighting croplands as the most vulnerable land-use class during monsoonal flooding [63]. However, unlike some national-scale assessments that emphasize a more balanced distribution of impacts across

land-use types, the disproportionately high agricultural impact in this study suggests a localized livelihood dependency effect, indicating that village-scale analyses may reveal sharper sectoral vulnerabilities that are often masked in coarser-resolution studies. The application of multi-sensor remote sensing (Sentinel-1 SAR and Sentinel-2 optical imagery) demonstrated high effectiveness in flood delineation, supporting findings that emphasize the advantages of SAR data in cloud-covered conditions [43]. However, while previous studies often report near-real-time operational efficiency, this study's integration with household-level data revealed temporal mismatches between satellite detection and ground-reported impacts. This contrasts with approaches that treat satellite-derived flood extent as a sufficient proxy for impact assessment, suggesting that remote sensing alone may underestimate prolonged socio-economic consequences. The strong spatial clustering observed in vulnerability indicators is consistent with geostatistical studies in flood-prone regions, which confirm that flood impacts are spatially non-random and concentrated. However, the moderate explanatory power of regression results ($R^2 = 0.12–0.13$) diverges from findings of higher predictive accuracy in machine learning-based susceptibility models. This discrepancy likely arises because the present study incorporates complex socio-economic variables, which introduce greater variability compared to purely physical parameters and reduce model predictability. Another important point of divergence relates to the role of topographic factors. While slope is often identified as a significant determinant of flood susceptibility [64], it was not statistically significant in this study. This inconsistency can be explained by the geomorphological uniformity of the study area, where minimal elevation variation reduces the influence of slope, and flood behavior is instead governed by proximity to the river and drainage inefficiencies. This highlights the importance of context-specific factor selection, as variables significant at broader scales may not hold relevance at localized levels. The findings further support the critical role of socio-economic vulnerability in shaping flood impacts. However, the magnitude of economic losses observed in this study—up to 75% income reduction and post-flood inflation exceeding 50%—appears more severe than those typically reported in broader-scale assessments. This suggests that localized economic shocks and market disruptions may intensify vulnerability beyond patterns identified in regional or global analyses. In contrast to studies advocating a shift toward nature-based and non-structural flood management approaches [65], the strong clustering of community preference for structural measures in this study indicates a continued reliance on hard engineering solutions [66]. This divergence highlights a gap between community-level adaptation preferences and evolving policy directions in sustainable flood risk management. Finally, the identification of distinct vulnerability hotspots supports findings from spatial hotspot analyses that confirm the localized nature of flood risk. However, unlike studies that treat hotspots as static zones, the integrated analysis in this research demonstrates that vulnerability is multi-dimensional and dynamically shaped by the interaction of physical, social, and economic factors. This suggests that single-indicator approaches may underestimate the true intensity and complexity of flood risk. In summary, while the study broadly aligns with existing literature, it also reveals important divergences related to scale, methodology, and socio-economic complexity. These findings emphasize the importance of integrated, village-scale approaches for capturing localized flood vulnerability patterns and highlight the need for combining geospatial technologies with ground-based socio-economic data to achieve a more comprehensive and context-sensitive understanding of flood risk.

Conclusion:

This study presents an integrated geospatial and geostatistical assessment of flood hazard and vulnerability along the Sutlej River floodplain in eastern Kasur, Pakistan. The 2025 flood inundated a total of 17 km^2, with agricultural land accounting for 87.18% of the affected area, followed by built-up land (4.45%), water bodies (3.01%), and barren land (1.73%). These figures demonstrate the disproportionate impact on agrarian livelihoods in low-lying rural settlements. Spatial analysis revealed statistically significant clustering of flood vulnerability indicators.

Household damage exhibited a Moran's I value of 0.29 ($p < 0.001$), agricultural land erosion 0.354 ($p < 0.000001$), and floodwater entry frequency 0.318 ($p < 0.001$), indicating that flood impacts are geographically concentrated rather than randomly distributed. Regression analysis further showed a positive relationship between spatial clustering and vulnerability indicators, with R^2 values of 0.1362 (Z-test) and 0.1235 (Moran's I), suggesting that spatial dependence partially explains observed vulnerability patterns. Socio-economic assessments revealed severe local impacts, including income reductions of up to 75% per household (PKR 250,000–400,000), significant crop losses, and localised post-flood price inflation exceeding 50%. Hotspot identification highlighted Sahgerah, Wallay Wala, Ullanke & Jumeke, Maste Ki, Chanda Singh Wala, and Nagar Amanpura as critical areas where physical, economic, and social vulnerabilities converge. Overall, the study demonstrates that integrating GEE-based multi-sensor remote sensing with household-level survey data, combined with geostatistical validation, provides a robust, village-scale framework for flood vulnerability assessment. This framework not only quantifies hazard extent and socio-economic impacts but also identifies spatially concentrated risk zones, supporting evidence-based and targeted disaster risk reduction strategies. The findings emphasize the importance of data-driven, spatially explicit, and multi-dimensional approaches for improving flood preparedness, resilience, and adaptive planning in highly flood-prone riverine regions like eastern Kasur.

Implications:

The study emphasizes the importance of evidence-based flood risk zoning and land-use planning in the Sutlej River floodplain. Agricultural areas and vulnerable settlements require targeted strategies, including risk-informed planning, flood-resilient agricultural practices, and adaptive compensation mechanisms. Identification of critical hotspots guides strategic infrastructure investments and early warning systems, ensuring that resources are prioritized for the most at-risk communities.

For disaster management, the research highlights the value of spatially explicit interventions, enabling authorities to focus relief, preparedness, and recovery efforts on high-risk areas rather than applying uniform measures. Insights into socio-economic vulnerability inform livelihood restoration, social protection programs, and efficient allocation of emergency resources, enhancing community resilience to future flood events. Methodologically, the study demonstrates the integration of multi-sensor remote sensing, geostatistical analysis, and household-level data as a robust framework for flood vulnerability assessment. This approach offers a replicable and scalable methodology for understanding spatial patterns of hazard and vulnerability, contributing to the broader literature on geospatially informed disaster risk assessment and planning.

Recommendations:

Based on the geostatistical and GEE-based assessment of flood vulnerability along the Sutlej River floodplain in eastern Kasur, the following recommendations are derived directly from the study's quantified results and prioritised according to the severity of impacts and socio-economic losses. The analysis identified Sahgerah, Huseen Khane, Wallay Wala, Ullanke & Jumeke, Maste Ki, Chanda Singh Wala, and Nagar Amanpura as the most critical hotspots, where floodwater inundation, household damage, and agricultural losses were highest. Quantified findings indicate:

Floodwater inundation affected 17 km^2, with agricultural land constituting 87.18% of the impacted area.

Household income losses reached up to 75% per household (PKR 250,000–400,000) in the most affected villages.

Agricultural land erosion and repeated floodwater entry were spatially clustered, with Moran's I values of 0.354 and 0.318, respectively, indicating concentrated vulnerability.

Structural and Infrastructural Measures (Highest Priority):

Housing Interventions: Retrofitting or rebuilding Katcha and Semi-Pucca houses in the identified hotspots should be prioritized to reduce household damage, especially in areas with the highest Moran's I for damage (0.29, $p < 0.001$).

Flood Control Structures: Construct and maintain embankments, spurs, and drainage channels in zones with repeated floodwater entry and agricultural erosion to protect both lives and livelihoods.

Institutional and Policy Actions (High Priority):

Establish community-based early warning systems and local communication units in hotspot villages to ensure rapid flood alerts.

Develop rescue outposts and emergency supply depots near high-impact areas to reduce response times.

Implement floodplain zoning and land-use regulations, particularly in villages with the largest economic losses and repeated inundation, to reduce long-term exposure.

Community Capacity Building (Medium Priority):

Conduct CBDRM programs emphasizing evacuation drills, first aid, and flood preparedness in villages with low awareness but high vulnerability indices.

Implement targeted awareness campaigns for agrarian communities, which constitute the majority of the affected area, highlighting climate-resilient agricultural practices and livelihood protection.

Long-Term Adaptation Strategies (Medium–Low Priority):

Plan relocation for settlements within the most severely impacted hotspots to reduce repeated flood exposure.

Promote adaptive and climate-resilient agriculture in flood-prone croplands to stabilize livelihoods and enhance long-term resilience.

By directly linking interventions to quantified flood extent, economic losses, and hotspot vulnerability indices, this prioritized approach ensures that structural, institutional, and community-based measures are spatially precise, socially inclusive, and aligned with the severity of impacts, supporting sustainable flood risk reduction in eastern Kasur.

References:

[1] A. David Raj and A. David Raj, "Climate Change Induced Hydro-Meteorological Extremes in the Himalayan Region," pp. 33–56, 2025, doi: 10.1007/978-3-031-85359-3_2.

[2] Dr Chrysanthus Chukwuma Sr, "Invariance of Extreme Hydrologic Events and Climate Change in the Risk Reduction on Environment and Health," *Greenfort Int. J. Appl. Med. Sci.*, vol. 3, no. 2, pp. 92–102, 2025, doi: 10.62046/gijams.2025.v03i02.011.

[3] Xiaojing Sun, Ruonan Li, "Assessment of climate change impacts and urban flood management schemes in central Shanghai," *Int. J. Disaster Risk Reduct.*, vol. 65, p. 102563, 2021, doi: https://doi.org/10.1016/j.ijdrr.2021.102563.

[4] Santiago X. Núñez Mejía, Santiago Mendoza Paz, "Climate change impacts on hydrometeorological and river hydrological extremes in Quito, Ecuador," *J. Hydrol. Reg. Stud.*, vol. 49, p. 101522, 2023, doi: https://doi.org/10.1016/j.ejrh.2023.101522.

[5] Andreas N. Angelakis, Andrea G. Capodaglio, "Evolution of Floods: From Ancient Times to the Present Times (ca 7600 BC to the Present) and the Future," *Land*, vol. 12, no. 6, p. 1211, 2023, doi: 10.3390/land12061211.

[6] Robindro Singh Khwairakpam; Sananda Kundu, "Enhanced flood quantile estimation and its implications in rainfall–discharge relationship during flood events in Brahmani-Baitarani River basin, India," *Water Pract. Technol.*, vol. 12, no. 1, pp. 192–222, 2026, doi: https://doi.org/10.2166/wpt.2026.190.

[7] Martina Angela Caretta, Rodrigo Fernandez, "Flooding Hazard and Vulnerability. An

Interdisciplinary Experimental Approach for the Study of the 2016 West Virginia Floods," *Front. water*, vol. 3, 2021, doi: https://doi.org/10.3389/frwa.2021.656417.

[8] Konstantinos M Andreadis, Oliver E J Wing, Emma Colven, Colin J Gleason, Paul D Bates and Casey M Brown, "Urbanizing the floodplain: global changes of imperviousness in flood-prone areas," *Environ. Res. Lett.*, vol. 17, no. 10, p. 104024, 2022, [Online]. Available: https://iopscience.iop.org/article/10.1088/1748-9326/ac9197

[9] M. M. Q. Mirza, "Climate change, flooding in South Asia and implications," *Reg. Environ. Chang. 2010 111*, vol. 11, no. 1, pp. 95–107, Dec. 2010, doi: 10.1007/S10113-010-0184-7.

[10] Shuainan Liu, Yang Liu, "Flood Risk Assessment in the Greater Bay Area Based on Multidimensional Dynamic Data," *Int. Arch. Photogramm. Remote Sens. Spat. Inf. Sci.*, pp. 189–195, 2025, doi: 10.5194/isprs-archives-XLVIII-4-W14-2025-189-2025.

[11] W. Duan and K. Takara, "Impacts of Climate and Human Activities on Water Resources and Quality: Integrated Regional Assessment," *Impacts Clim. Hum. Act. Water Resour. Qual. Integr. Reg. Assess.*, pp. 1–183, Jan. 2020, doi: 10.1007/978-981-13-9394-5/COVER.

[12] S. Srivastava, T. Gerdes, and T. Roy, "County-scale flood risk assessment of properties and associated population in the United States," *Nat. Hazards*, vol. 121, no. 3, pp. 2641–2664, Feb. 2025, doi: 10.1007/S11069-024-06892-8.

[13] "Climate change and water security in the Indo-Pacific region: Risks, responses, and a framework for action | Asia and the Pacific Water Resilience Hub." Accessed: Apr. 07, 2026. [Online]. Available: https://hub4r.adb.org/index.php/node/1421

[14] Abid Nazir, Awais Ahmad, "Flood-Induced Agricultural Damage Assessment: A Case Study of Pakistan," *Water*, vol. 17, no. 21, p. 3060, 2025, doi: https://doi.org/10.3390/w17213060.

[15] B. B. Shreevastav, "Flood Scenario and its Risk Management, Policy, Practices in Nepal," *Int. J. Sci. Eng. Res.*, vol. 10, no. 4, pp. 571–581, Apr. 2019, doi: 10.14299/IJSER.2019.04.07.

[16] A. Inam *et al.*, "The Geographic, Geological, and Oceanographic Setting of the Indus River – An Update," *Large Rivers Geomorphol. Manag.*, pp. 488–520, Apr. 2022, doi: 10.1002/9781119412632.CH17.

[17] Leanne Hauptman, Diana Mitsova, "Hurricane Ian Damage Assessment Using Aerial Imagery and LiDAR: A Case Study of Estero Island, Florida," *J. Mar. Sci. Eng*, vol. 12, no. 4, p. 668, 2024, doi: https://doi.org/10.3390/jmse12040668.

[18] Mustafa Javed, Jürgen Böhner & Shabeh ul Hasson, "Streamflow projections for the Jhelum River basin under climate change," *Discov. Appl. Sci.*, vol. 7, 2025, [Online]. Available: https://link.springer.com/article/10.1007/s42452-025-06721-y

[19] S. Haider, M. U. Masood, A. A. Awan, R. Z. N. Khan, and M. Rashid, "Understanding Climate Change Impacts on Coastal Communities: Resilience, Adaptation, and Sustainable Development in Sindh, Pakistan," pp. 391–423, 2025, doi: 10.1007/978-981-96-1733-3_18.

[20] "A historical appraisal of the water dispute in the Indus Basin, 1947-1960 - UUM Electronic Theses and Dissertation [eTheses]." Accessed: Mar. 26, 2026. [Online]. Available: https://etd.uum.edu.my/8713/

[21] Y. V. S. Bhageerath, A. V. S. Babu, K. H. V. D. Rao, K. Sreenivas, and P. Chauhan, "Flood period estimation using multi-sensor satellite data: Case study on Punjab floods 2023," *J. Earth Syst. Sci. 2025 1341*, vol. 134, no. 1, pp. 43-, Feb. 2025, doi: 10.1007/S12040-024-02499-6.

[22] D. Glover, "Exploring the Resilience of Bt Cotton's 'Pro-Poor Success Story,'" *Dev.*

Change, vol. 41, no. 6, pp. 955–981, Dec. 2010, doi: 10.1111/J.1467-7660.2010.01667.X;ISSUE:ISSUE:DOI.

[23] "Floods: Governance Challenges and the Roots of Repeated Climate Disasters in Pakistan (part II) – SLD." Accessed: Mar. 26, 2026. [Online]. Available: https://sld.com.pk/2025/07/24/floods-governance-challenges-and-the-roots-of-repeated-climate-disasters-in-pakistan-part-ii/

[24] R. Looney, "Economic impacts of the floods in Pakistan," *Contemp. South Asia*, vol. 20, no. 2, pp. 225–241, Jun. 2012, doi: 10.1080/09584935.2012.670203.

[25] S. Kondapalli, "The geo-politics of the Indo-Pacific: Perceptions, opportunities, and challenges," *New World Polit. Indo-Pacific Perceptions, Policies Interes.*, pp. 16–33, Jun. 2024, doi: 10.4324/9781003479307-3/GEO-POLITICS-INDO-PACIFIC-SRIKANTH-KONDAPALLI.

[26] UNDRR (United Nations Office for Disaster Risk Reduction), "Global Assessment Report on Disaster Risk Reduction (GAR)," 2022, [Online]. Available: https://www.undrr.org/gar

[27] I. Khan, A. Ullah, A. Z. Zaidi, and V. Panhwar, "Assessing glacial lake outburst flood potential using geospatial techniques: a case study of western part of Gilgit-Baltistan, Pakistan," *Arab. J. Geosci. 2022 161*, vol. 16, no. 1, pp. 1–12, Dec. 2022, doi: 10.1007/S12517-022-11088-0.

[28] Peng Cui, Nazir Ahmed Bazai, Zou Qiang, Wang Jiao, Wang Yan, Qingsong Xu, Lei Yu & Zhang Bo, "Flood risk assessment with machine learning: insights from the 2022 Pakistan mega-flood and climate adaptation strategies," *npj Nat. hazards*, 2025, [Online]. Available: https://www.nature.com/articles/s44304-025-00096-1

[29] M. R. Akram, "Transboundary flood and drought challenges: a case study of the Sutlej River in Pakistan," *Int. J. River Basin Manag.*, Jun. 2025, doi: 10.1080/15715124.2025.2512955.

[30] "Spatial Analysis of Urban Flood Vulnerability Using Weighted Overlay Technique For Identification of Hazard Zones In Greater Jakarta." Accessed: Mar. 26, 2026. [Online]. Available: https://www.researchgate.net/publication/392691295_Spatial_Analysis_Of_Urban_Flood_Vulnerability_Using_Weighted_Overlay_Technique_For_Identification_Of_Hazard_Zones_In_Greater_Jakarta

[31] M. Aliyu, A. A. Dandajeh, S. B. Igboro, and N. I. Abdullahi, "Flood Hazard Assessment and Mapping in River-Rima Floodplain, Birnin Kebbi-Nigeria," *Niger. J. Technol. Dev.*, vol. 22, no. 1, pp. 279–293, Mar. 2025, doi: 10.4314/NJTD.V22I1.2862.

[32] M. M. Islam, S. Matsushita, R. Noguchi, and T. Ahamed, "A damage-based crop insurance system for flash flooding: a satellite remote sensing and econometric approach," *Asia-Pacific J. Reg. Sci. 2021 61*, vol. 6, no. 1, pp. 47–89, Nov. 2021, doi: 10.1007/s41685-021-00220-9.

[33] Mohammad Zahednia, Shirin Shirazian, "Identifying the causes of floods and assessing the resulting environmental damage to provide a flood compensation model," *Anthropog. Pollut.*, vol. 9, no. 1, 2025, [Online]. Available: https://oiccpress.com/ap/article/view/17277

[34] P. Mishra and S. K. Prasad, "Lightweight Hybrid Deep Learning and Fuzzy-AHP Framework for Predictive Flood Susceptibility Mapping in the Ghaghara River Basin, India: A Data-Driven Approach for Enhanced Spatiotemporal Precision and Risk Prediction," *Earth Syst. Environ. 2026*, pp. 1–28, Jan. 2026, doi: 10.1007/S41748-025-00970-Y.

[35] Rakhee Ramachandran, Yadira Bajón Fernández, "Accuracy Assessment of Surveying Strategies for the Characterization of Microtopographic Features That Influence

Surface Water Flooding," *Remote Sens.*, vol. 15, no. 7, p. 1912, 2023, doi: 10.3390/rs15071912.

[36] S. Puttinaovarat, A. Saeliw, S. Pruitikanee, J. Kongcharoen, S. Chai-Arayalert, and K. Khaimook, "Flood Damage Assessment Geospatial Application Using Geoinformatics and Deep Learning Classification," *Int. J. Interact. Mob. Technol.*, vol. 16, no. 21, pp. 71–97, 2022, doi: 10.3991/ijim.v16i21.34281.

[37] Aslam A. Al-Omari, Nawras N. Shatnawi, "Utilizing Remote Sensing and GIS Techniques for Flood Hazard Mapping and Risk Assessment," *Civ. Eng. J.*, vol. 10, no. 5, 2024, [Online]. Available: https://www.civilejournal.org/index.php/cej/article/view/4836

[38] M. A. R. Khan, M. A. Rouf, N. Sultana, and M. S. Akter, "Development of A Fog Computing-Based Real-Time Flood Prediction And Early Warning System Using Machine Learning And Remote Sensing Data," *J. Sustain. Dev. Policy*, vol. 01, no. 01, pp. 144–169, Mar. 2025, doi: 10.63125/6y0qwr92.

[39] Y. Hasnaoui *et al.*, "Integrated Remote Sensing and Deep Learning Models for Flash Flood Detection Based on Spatio-temporal Land Use and Cover Changes in the Mediterranean Region," *Environ. Model. Assess. 2025 305*, vol. 30, no. 5, pp. 1013–1035, May 2025, doi: 10.1007/s10666-025-10035-z.

[40] C. Campo, P. Tamagnone, S. Choy, T. D. Tran, G. J.-P. Schumann, Y. Kuleshov, "Monitoring Flood Inundation Dynamics From Space," *Rev. Geophys.*, 2026, doi: https://doi.org/10.1029/2025RG000885.

[41] S. Martinis, M. Wieland, M. Rattich, C. Bohnke, and T. Riedlinger, "Automatic Near-Real Time Flood Extent and Duration Mapping based on Multi-Sensor Earth Observation Data," *Int. Geosci. Remote Sens. Symp.*, pp. 3243–3246, Sep. 2020, doi: 10.1109/IGARSS39084.2020.9324295.

[42] Sona Guliyeva & Piero Boccardo, "Geospatial Technologies for Flood and Drought Management: A Review of Earth Observation Data, Procedures, and their Operational Effectiveness," *Aerotec. Missili Spaz.*, 2026, [Online]. Available: https://link.springer.com/article/10.1007/s42496-026-00309-4

[43] Angelica Tarpanelli, Christian Massari, Beatriz Revilla-Romero, Mohammad J. Tourian, "The Potential of EO Data for Enhanced Flood Monitoring and Forecasting: A Consortium Assessment," *Surv. Geophys.*, vol. 47, pp. 317–358, 2026, [Online]. Available: https://link.springer.com/article/10.1007/s10712-026-09935-w

[44] M. S. Mirza Waleed, "High-resolution flood susceptibility mapping and exposure assessment in Pakistan: An integrated artificial intelligence, machine learning and geospatial framework," *Int. J. Disaster Risk Reduct.*, vol. 121, p. 105442, 2025, doi: https://doi.org/10.1016/j.ijdrr.2025.105442.

[45] Xiaoyi Liu, Hichem Sahli, "Flood Inundation Mapping from Optical Satellite Images Using Spatiotemporal Context Learning and Modest AdaBoost," *Remote Sens.*, vol. 9, no. 6, p. 617, 2017, doi: https://doi.org/10.3390/rs9060617.

[46] Yayi Zhang, Yongqiang Wei, "Data Uncertainty of Flood Susceptibility Using Non-Flood Samples," *Remote Sens.*, vol. 17, no. 3, p. 375, 2025, doi: 10.3390/rs17030375.

[47] Tianlian Wang, Zhiyuan Fu, "Deep learning for decoding climate–urbanization synergies: flood susceptibility forecasting under SSP-RCP scenarios in Beijing, China," *J. Hydrol.*, vol. 672, 2026, doi: 10.1016/j.jhydrol.2026.135364.

[48] Velasquez Hurtado, Wilson Andres, "Data Fusion and change detection techniques based on optical and Synthetic Aperture Radar satellite imagery for damage mapping and multi-temporal assessment of the recovery and reconstruction process after natural disasters," *Tesi di dottorato*, 2026, [Online]. Available: https://tesidottorato.depositolegale.it/handle/20.500.14242/357518

[49] Antonika Shapovalova, "Flood Radar: Multi-Sensor SAR-Based Flood Mapping and Evacuation Modeling — A Case Study of the July 2025 Texas Flood," *Researchgate*, 2025, [Online]. Available: https://www.researchgate.net/publication/397419938_Flood_Radar_Multi-Sensor_SAR-Based_Flood_Mapping_and_Evacuation_Modeling_-_A_Case_Study_of_the_July_2025_Texas_Flood

[50] M. A. Al Sayeem and R. B. Rahman, "A Cloud-Based Sentinel-1 SAR and Sentinel-2 Optical Approach for Rapid Flood Mapping and Impact Assessment: Application to the 2022 Sylhet District Flood, Bangladesh," 2026, doi: 10.2139/SSRN.6142670.

[51] Benedikt Mester, Katja Frieler, "Socioeconomic predictors of vulnerability to flood-induced displacement," *Nat. Commun.*, vol. 16, 2025, [Online]. Available: https://pmc.ncbi.nlm.nih.gov/articles/PMC12441118/

[52] Bingyan Ma, Jing Guo, "Comprehensive risk assessment of urban floods based on flood simulation and socio-economic vulnerability," *Front. Earth Sci.*, vol. 13, 2025, doi: https://doi.org/10.3389/feart.2025.1645693.

[53] Muhammad Ahsan Mukhtar, Donghui Shangguan, "Integrated flood risk assessment in Hunza-Nagar, Pakistan: unifying big climate data analytics and multi-criteria decision-making with GIS," *Front. Enviromental Sci.*, vol. 12, 2024, doi: https://doi.org/10.3389/fenvs.2024.1337081.

[54] Chengjie Zhou, Hanru Shen, "A spatial-explicit analysis of influencing factors of observed floods in the Yangtze River Delta, China," *Landsc. Ecol.*, vol. 40, no. 9, 2025, doi: 10.1007/s10980-025-02201-1.

[55] H. Uyguçgil, "Rapid Flash Flood Mapping Using Sentinel-1 SAR Data on the Google Earth Engine Platform," *Int. J. Environ. Geoinformatics*, vol. 4, no. 12, pp. 408–414, Jan. 2026, doi: 10.26650/ijegeo.1650297.

[56] F. Arshad *et al.*, "Indigenous farmer's perception about fodder and foraging species of Semi-arid lowlands of Pakistan: A case study of District Kasur, Pakistan," *Taiwania*, vol. 67, no. 4, pp. 510–523, 2022, doi: 10.6165/TAI.2022.67.510.

[57] Muhammad Waheed, Shiekh Marifatul Haq, "Grasses in Semi-Arid Lowlands—Community Composition and Spatial Dynamics with Special Regard to the Influence of Edaphic Factors," *Sustainability*, vol. 14, no. 22, p. 14964, 2022, doi: 10.3390/su142214964.

[58] Muhammad Saiful Ruuhulhaq, Arif Rohman, "Exploring Google Earth Engine for Flood Detection (A Case Study in Bandung City)," *Int. J. Disaster Dev. Interface*, vol. 5, no. 1, pp. 223–245, 2025, doi: 10.53824/ijddi.v5i1.93.

[59] B. Bilal, R. Saleemi, A. Amer, and H. Gulzar, "Remote Sensing and Machine Learning-Driven Flood Inundation Mapping of September 2025 Ravi Watershed Using Sentinel-1 SAR," *Int. J. Innov. Sci. Technol.*, vol. 7, no. 4, pp. 2338–2350, 2025, Accessed: Apr. 07, 2026. [Online]. Available: https://ideas.repec.org/a/abq/ijist1/v7y2025i4p2338-2350.html

[60] "Sentinel-1 – Documentation." Accessed: Apr. 07, 2026. [Online]. Available: https://documentation.dataspace.copernicus.eu/Data/SentinelMissions/Sentinel1.html

[61] N. Gorelick, M. Hancher, M. Dixon, S. Ilyushchenko, D. Thau, and R. Moore, "Google Earth Engine: Planetary-scale geospatial analysis for everyone," *Remote Sens. Environ.*, vol. 202, pp. 18–27, Dec. 2017, doi: 10.1016/J.RSE.2017.06.031.

[62] A. M. Abdi, "Land cover and land use classification performance of machine learning algorithms in a boreal landscape using Sentinel-2 data," *GIScience Remote Sens.*, vol. 57, no. 1, pp. 1–20, Jan. 2020, doi: 10.1080/15481603.2019.1650447.

[63] Afshin Akram, Arifa Tahir, "GIS based flood extent assessment using MODIS

satellite remote sensing and spatial analysis," *Front. Earth Sci.*, vol. 12, 2024, doi: https://doi.org/10.3389/feart.2024.1309629.

[64] Rana Muhammad Amir Latif, Jinliao He, "Flood Susceptibility Mapping in Punjab, Pakistan: A Hybrid Approach Integrating Remote Sensing and Analytical Hierarchy Process," *Atmosphere (Basel).*, vol. 16, no. 1, p. 22, 2025, doi: https://doi.org/10.3390/atmos16010022.

[65] Tania Islam, Ethiopia B. Zeleke, Mahmud Afroz, "A Systematic Review of Urban Flood Susceptibility Mapping: Remote Sensing, Machine Learning, and Other Modeling Approaches," *Remote Sens*, vol. 17, no. 3, p. 524, 2025, doi: https://doi.org/10.3390/rs17030524.

[66] Izhar Ahmad, Rashid Farooq, Muhammad Ashraf, Muhammad Waseem & Donghui Shangguan, "Improving flood hazard susceptibility assessment by integrating hydrodynamic modeling with remote sensing and ensemble machine learning," *Nat. Hazards*, vol. 121, 2025, [Online]. Available: https://link.springer.com/article/10.1007/s11069-025-07109-2